



# DIGITAL ACCESS TO SCHOLARSHIP AT HARVARD

## CD1a autoreactive T cells recognize natural skin oils that function as headless antigens

The Harvard community has made this article openly available.  
[Please share](#) how this access benefits you. Your story matters.

<b>Citation</b>	de Jong, A., T. Cheng, S. Huang, S. Gras, R. W. Birkinshaw, A. Kasmar, I. van Rhijn, et al. 2014. "CD1a autoreactive T cells recognize natural skin oils that function as headless antigens." <i>Nature immunology</i> 15 (2): 177-185. doi:10.1038/ni.2790. <a href="http://dx.doi.org/10.1038/ni.2790">http://dx.doi.org/10.1038/ni.2790</a> .
<b>Published Version</b>	<a href="https://doi.org/10.1038/ni.2790">doi:10.1038/ni.2790</a>
<b>Accessed</b>	February 16, 2015 9:29:44 PM EST
<b>Citable Link</b>	<a href="http://nrs.harvard.edu/urn-3:HUL.InstRepos:12785975">http://nrs.harvard.edu/urn-3:HUL.InstRepos:12785975</a>
<b>Terms of Use</b>	This article was downloaded from Harvard University's DASH repository, and is made available under the terms and conditions applicable to Other Posted Material, as set forth at <a href="http://nrs.harvard.edu/urn-3:HUL.InstRepos:dash.current.terms-of-use#LAA">http://nrs.harvard.edu/urn-3:HUL.InstRepos:dash.current.terms-of-use#LAA</a>

*(Article begins on next page)*

Published in final edited form as:

Nat Immunol. 2014 February ; 15(2): 177–185. doi:10.1038/ni.2790.

## CD1a autoreactive T cells recognize natural skin oils that function as headless antigens

Annemieke de Jong<sup>1,8,9</sup>, Tan-Yun Cheng<sup>1,8</sup>, Shouxiong Huang<sup>1</sup>, Stephanie Gras<sup>5</sup>, Richard W. Birkinshaw<sup>5</sup>, Anne Kasmar<sup>1</sup>, Ildiko van Rhijn<sup>1,6</sup>, Victor Peña-Cruz<sup>3</sup>, Daniel T. Ruan<sup>2</sup>, John D. Altman<sup>4</sup>, Jamie Rossjohn<sup>5,7</sup>, and D. Branch Moody<sup>1,9</sup>

<sup>1</sup>Division of Rheumatology, Immunology and Allergy <sup>2</sup>Department of Gastrointestinal and General Surgery, Brigham and Women's Hospital, Harvard Medical School <sup>3</sup>Boston University, Boston MA <sup>4</sup>Emory Vaccine Center, Atlanta GA <sup>5</sup>Department of Biochemistry and Molecular Biology, School of Biomedical Sciences, Monash University, Clayton, Australia <sup>6</sup>Department of Infectious Diseases and Immunology, Faculty of Veterinary Medicine, Utrecht University, Utrecht, The Netherlands <sup>7</sup>Institute of Infection and Immunity, Cardiff University, School of Medicine, Heath Park, Cardiff CF14 4XN, UK

### Abstract

CD1a autoreactive T cells are common in human blood and skin, but the search for natural autoantigens has been confounded by background T cell responses to CD1 proteins and self lipids. After capturing CD1a-lipid complexes, we gently eluted ligands, while preserving unliganded CD1a for testing lipids from tissues. CD1a released hundreds of ligands of two types. Inhibitory ligands were ubiquitous membrane lipids with polar headgroups, whereas stimulatory compounds were apolar oils. CD1a autoantigens naturally accumulate in epidermis and sebum, where they were identified as squalene and skin waxes. T cell activation by skin oils suggests that headless mini-antigens nest within CD1a and displace non-antigenic resident lipids with large head groups. Oily autoantigens naturally coat the skin's surface, pointing to a new mechanism of barrier immunity.

### Introduction

T cell autoreactivity to CD1 was first described for an  $\alpha\beta$  T cell clone recognizing CD1a<sup>1</sup>, leading to a search for self-antigens that might bind to CD1 proteins. Although most research has focused on CD1d and NKT cells, recent studies that measure T cell autoreactivity to each type of human CD1 antigen presenting molecule have identified the highest rates of recognition of CD1a or CD1c<sup>2,3</sup>. CD1a- or CD1c-autoreactive cells infiltrate thyroid glands in autoimmune disease<sup>4</sup>. Also, human CD1a-autoreactive T cells in the blood

Users may view, print, copy, download and text and data- mine the content in such documents, for the purposes of academic research, subject always to the full Conditions of use: [http://www.nature.com/authors/editorial\\_policies/license.html#terms](http://www.nature.com/authors/editorial_policies/license.html#terms)

<sup>9</sup>Correspondence should be addressed to D.B.M (bmoody@partners.org) or AdJ (ad2952@columbia.edu).

<sup>8</sup>These authors contributed equally to this work

Current affiliation AdJ: Department of Dermatology, Columbia University Medical Center, New York NY

#### Author contributions

A.d.J. and D.B.M. designed research and wrote the manuscript. A.d.J. and T-Y.C. designed and performed experiments. A.K. performed CD1a pull-down assay and contributed to cell-free assays. S.H. performed acid stripping and CD1 eluent reloading for T cell activation, elution and Q-TOF mass spectrometry of CD1a ligands. V.P-C. provided epidermal sheets for lipid extraction. D.T.R. provided thyroid tissue samples. J.D.A. provided biotinylated CD1a monomers. I.V.R. determined alleles of TCR alpha and beta chains. S.G., R.W.B., and J.R. designed experiments and contributed surface plasmon resonance data. J.R. assisted in preparation of the manuscript.

express cutaneous lymphocyte antigen, CCR4, CCR6, CCR10, which mediate migration to skin<sup>2</sup>. Colocalization of CD1a-expressing Langerhans cells (LCs) and CD1a autoreactive T cells suggest basic roles for CD1a in skin immunity<sup>5</sup>.

Mammalian lipids that stimulate autoreactive T cells have been identified<sup>6-10</sup>. Many of these lipids were selected for study because they mimic foreign  $\alpha$ -galactosyl ceramide antigens for NKT cells<sup>7,8,10</sup>, whereas others were pre-selected and then used to expand populations of T cells through repeated *in vitro* immunization<sup>6,11</sup>. An approach using unimmunized T cells to analyze the many types of endogenous lipids expressed in the tissues where T cells reside is desirable because this discovery process is unbiased and focuses on natural antigens. However, endogenous antigens within antigen presenting cells (APCs) cause background T cell activation that masks T cell response to added lipids in reconstitution assays. Here we used several techniques to defeat such background signals and identified oily autoantigens that lack carbohydrate or charged headgroups. Discovery of antigens lacking polar headgroups was unexpected because known antigens presented by MHC<sup>12,13</sup> and CD1<sup>14</sup> use hydrogen bonding and ionic interactions to bind TCRs. Lacking any precedent for TCR recognition of oils, we used structure-function assays and analysis of hundreds of ligands released from CD1a proteins to identify general patterns of antigens that stimulated CD1a autoreactivity. Whereas lipids with hydrophilic headgroups were inhibitory, several lipids lacking headgroups stimulated T cells. We proposed that small, headless molecules nest within the CD1 groove are recognized based on non-interference of TCR contact with CD1.

## Results

### Polyclonal T cells show autoreactivity to CD1a

Recently developed methods measure autoreactivity of T cells to CD1a, CD1b, CD1c and CD1d using CD1 transfected K562 cells<sup>2</sup>. These MHC<sup>low</sup> cells function as universal APCs that bypass alloreactivity and detect polyclonal CD1 autoreactive cells *ex vivo* in any donor. In agreement with our prior study of 14 donors using interferon- $\gamma$  (IFN- $\gamma$ ) as a readout<sup>2</sup>, we detected high rates of CD1a autoreactivity in a new analysis of short term T cell lines using IL-2 release. CD1a<sup>+</sup> APCs generated detectable autoreactivity in 8 out of 10 patients. As compared to other CD1 isoforms, CD1a generated the highest responses in 7 of 10 donors (Fig. 1a). These results, along with evidence that CD1a autoreactive cells can comprise up to 10 percent of all T cells<sup>3</sup>, prompted us to focus on autoantigen discovery in the CD1a system, as the most prominent source of CD1 autoreactive T cells in human blood. We derived and named 5 T cell lines (BC2, DermT, BC5, Bgp, BC14) whose activation was inhibited by anti-CD1a blocking antibody (OKT6), confirming that the response was dependent on CD1a and not on other cell surface determinants (Fig. 1b).

### Isolation of antigenic CD1a complexes from cells

If autoantigens are present in the APCs, CD1 autoreactive T cells show baseline reactivity, which masks responses to any added antigen used in reconstitution assays. Background signals have been a major impediment to discovery of endogenous autoantigens, but might be overcome by dissociating CD1 proteins from the cells that produce them and stripping proteins of endogenously loaded ligands. Also, lipids eluting from CD1a proteins might reflect the types of lipids normally loaded onto CD1 proteins in cells, allowing identification of both non-stimulatory ligands and stimulatory autoantigens. Taking advantage of constructs previously designed for other CD1 proteins, we produced transmembrane-truncated, biotinylated CD1a proteins zippered to  $\beta$ -2 microglobulin ( $\beta$ <sub>2</sub>M) with high yields in HEK293 cells<sup>15,16</sup> (Fig. 2a). These proteins showed the expected apparent mass and were pulled down by streptavidin beads (Fig. 2a). When bound to a plate, cell-derived CD1a

activated the CD1a-autoreactive T cell line BC2 (Fig. 2b). Thus the recombinant CD1a proteins retained the structures needed for activating T cells, creating an APC-free system for identifying antigens.

CD1a autoreactivity might occur due to TCR contact with unliganded CD1 proteins or CD1 proteins bound to ubiquitous self-molecules<sup>17</sup>. Dideoxymycobactin (DDM) is CD1a ligand that is known to bind within the A' and F' pockets of the groove<sup>18</sup> and to activate the T cell line CD8-2<sup>19</sup>. DDM suppressed BC2 activation in a dose-dependent fashion. Because culture wells were washed after adding lipid but before adding T cells, inhibition was unlikely due to non-specific effects of lipid on T cells. Lack of toxicity was further supported when DDM activated CD8-2 over the same dose range at which inhibition of BC2 was seen (Fig. 2c). Thus, BC2 activation likely involved the distal surface of CD1a near the groove portal, where DDM binds. However, whether DDM displaced an antigenic self-compound or inserted into the groove to block TCR contact with the previously unliganded CD1a remained unresolved.

Unloading of ligands occurs over a pH range of 6.5 to 4, which represents conditions that do not induce irreversible unfolding of CD1a proteins<sup>20</sup>. Brief pretreatment of plate-bound CD1a proteins with acidic pH (Supplementary Fig. 1), followed by washing at neutral pH, diminished CD1a stimulation of BC2, suggesting that ligand loss abrogated T cell activation, pointing away from direct recognition of unliganded CD1a proteins as the mechanism of T cell activation. By producing CD1a and MHC class I proteins in high yield, eluting ligands under mildly acidic conditions and applying concentrated eluents to pre-stripped CD1a proteins, we could demonstrate transfer of stimulatory substances from CD1a to CD1a but not MHC class I to CD1a (Fig. 2d). Thus, endogenous autoantigens exist and are loaded onto CD1a proteins by the cells that produce them.

### Cellular CD1a protein complexes bind the T cell receptor (TCR)

To understand the basis of BC2 TCR autoreactivity towards CD1a, we expressed the ectodomains of the BC2 TCR  $\alpha$  and  $\beta$  chains and measured the affinity of the BC2 TCR towards to the U293-derived truncated CD1 proteins using surface plasmon resonance (SPR). The autoreactive BC2 TCR bound to CD1a proteins derived from cells (Fig. 2e) with an affinity value ( $K_d = 92.7 \pm 5.3 \mu\text{M}$ ) that is comparable to that seen in autoreactive TCR-peptide-MHC interactions<sup>21</sup>. Thus, the BC2 TCR can bind to cellular CD1a complexes.

### CD1a releases chemically diverse cellular ligands

Next, we attempted to identify both antigenic and non-antigenic ligands that eluted from CD1a in chloroform and methanol. Prior studies of CD1d<sup>22,23</sup>, CD1c<sup>24</sup> and CD1b<sup>25</sup> identified large numbers of lipid ligands binding to CD1 proteins. However, the identity of CD1a ligands was unknown. Transmembrane truncation can influence some lipids bound to CD1d proteins<sup>23</sup> and necessarily removes cytoplasmic sequences with tail motifs that mediate recycling to endosomes. However, human CD1a lacks recycling motifs<sup>26</sup>, so would be expected to mimic non-recycled full length CD1a, as supported by a detailed study comparing native and tail-truncated truncated CD1a proteins<sup>27</sup>. Analysis of eluents using sensitive methods of nanoelectrospray infusion mass spectrometry detected more than one hundred distinct ions with  $m/z$  values between 700 and 1500, indicating that many self-molecules bind to CD1a (Fig. 3a). Focusing on intense ions in the positive mode, collision-induced dissociation mass spectrometry (CID-MS) identified four types of sphingolipid ligands: sphingomyelin, trihexosylceramide, ganglioside GM3 and globoside Gb4. In addition, we detected trace signals for triacylglyceride TAG (Fig. 3a and Supplementary Fig. 2). In negative mode analysis, we identified five classes of phosphatidic acid containing compounds: phosphatidylinositol (PI), phosphatidylethanolamine (PE), phosphatidylglycerol

(PG), phosphatidylserine (PS), and phosphatidylcholine (PC) (Fig. 3a and Supplementary Fig. 3). Within each class we detected a range of molecular variants that differ in chain length and unsaturation. Overall, CD1a proteins normally bind a broad range of molecules that differ in the nature of their hydrophilic head groups, which can contain carbohydrates, charged atoms, or in the case of TAG, lack polar head groups.

To better quantitate the molecular heterogeneity of CD1a ligands, we took advantage of a recently developed lipidomics platform<sup>25,28</sup> which detected 1,336 molecular events. In the normal phase, retention time correlates with polarity. Using named molecules within this dataset (TAG, DAG, PE, SM) as benchmarks, we classified CD1a eluted molecular events into 3 groups based on retention time. CD1a ligands distribute somewhat evenly into groups described as having low (22%), intermediate (31%) or high (47 %) polarity (Fig. 3c). Thus, truncated CD1a proteins egressing through the secretory pathway normally bind hundreds of distinct ligands that span a broad spectrum of polarity.

### Triacylglyceride is an autoantigen

CD1a protein overexpression did not produce adequate lipid yield for complex separation approaches needed to identify the antigenic substances within eluents. Therefore, we diverted from the goal of assessing only natural cellular molecules and assembled a panel of synthetic or purified lipid standards that approximated or matched the structures of eluted natural compounds (Fig. 3b) or known antigens, such as sulfatide, PI and PE. Among diverse glycolipids, phospholipids, sulfolipids and sphingolipids tested, we observed stimulatory responses only to synthetic triacylglyceride (TAG) with C16:1 fatty acids, defining this molecule as an autoantigen for CD1a (Fig. 3d). This finding was surprising because TAG lacks a bulky or polar headgroup, whereas most or all previously known antigens carry carbohydrate, phosphate or other rigid and polar or charged hydrophilic groups, which interact with TCRs. Many glycolipids or phospholipids, including sphingomyelin and phosphatidylcholine, strongly inhibited the baseline T cell response to CD1a (Fig. 3d). This inhibition likely reflected lipids binding to CD1a rather than non-specific effects on T cells, because excess lipid is washed prior to adding T cells. Thus, naturally occurring CD1a ligands, especially polar lipids with charged or large carbohydrate groups are not merely ignored, but instead act as antagonists that inhibit autoreactivity of BC2.

### Differential autoreactivity of human tissues

In contrast to the ubiquitous expression on MHC class I, CD1a is only expressed on tissue resident DCs and is constitutively expressed at extremely high density on epidermal LCs<sup>29,30</sup>. This restricted tissue distribution suggests a plausible means of restricting autoreactive T cell activation based on physical separation of T cells and CD1a-expressing APCs, as proposed recently<sup>2,5</sup>. The CD1a reconstitution system allowed testing of the segregation hypothesis by detecting T cell responses to lipid extracts of various tissues and type-specific cells. Lipid extracts made with chloroform/methanol from PBMC, K562 cells, transformed B cells (C1R), myeloid cells (THP-1), and thyroid tissue failed to detectably activate BC2 and usually showed dose-dependent inhibition below baseline activation thresholds (Fig. 4a). However, lipid extracts of human epidermis activated BC2 in a dose-dependent manner. Our initial screens of purified lipids suggested that BC2 responds to synthetic triacylglycerides (TAG), and the human epidermis is highly enriched in TAG<sup>31</sup>. Therefore, we hypothesized that the relatively selective response to skin might be mediated by this tissue's natural enrichment for TAG or related apolar lipids.

Normal phase silica thin layer chromatography (TLC) separates lipids based on polarity, so hydrophobic lipids show higher retention factors (Rf)<sup>32</sup>. As expected, the TLC analysis of

tissue extracts showed that the profile of lipids from epidermis was markedly skewed towards apolar lipids (Fig. 4b). As compared to other cell types, epidermis contained more intense spots matching TAG standards and relatively less intense spots matching PC and SM, which acted as T cell antagonists when tested as purified molecules (Fig. 3d, 4b).

We next tested whether the strong activation of BC2 by epidermis resulted from its relatively high production of the unusually hydrophobic lipids. Therefore, we extracted epidermis with a non-polar solvent, pure chloroform. As compared to extracts made with a mixture of chloroform and methanol, TLC showed that the chloroform-extracted lipid profile skewed towards more hydrophobic lipids, including TAG, cholesterol esters and wax esters (Fig. 4b). Indeed, extracts made with pure chloroform showed enhanced BC2 activation by epidermal lipids from all three human donors tested (Fig. 4c). Whereas chloroform and methanol extracts of K562, THP-1 and thyroid tissues were inhibitory, chloroform extraction of the same tissues yielded extracts with net T cell activating effects. Thus, different human tissues have differing antigenic potency, which is directly correlated with the ratio of apolar to polar lipids present. It is notable that epidermis shows the highest degree of antigenicity, because human skin is where CD1a<sup>+</sup> epidermal LCs are localized and is enriched for CD1a autoreactive T cells<sup>2</sup>.

### Identification of endogenous cellular autoantigens

Building on identification of synthetic TAG as an autoantigen (Fig. 3d) and the correlation of TAG content with the antigenic potency of tissues (Fig. 4), we sought to directly purify the natural autoantigen(s) from epidermis. Using a solvent system that separates highly apolar lipids<sup>32</sup>, preparative TLC plates were sprayed with water to visualize the most abundant lipid bands (0, 1, 2, 3, 4). The silica between each band (0-1, 1-2, 2-3, 3-4, 4+) was scraped in attempt to recover lipids produced at lower concentrations. We preserved a slice of the plate for charring to reveal the location of natural skin lipids in comparison to authentic standards (Fig. 5a). As predicted, analysis of epidermal lipids showed a T cell response to band 3, which comigrated with a TAG standard. Thus, natural (Fig. 5b) and synthetic TAGs (Fig. 3d) are CD1a autoantigens.

### Patterns of autoantigen recognition in tissues

Prior efforts to identify antigens that activate one T cell clone typically yield a single kind of stimulatory molecule, recognized without cross-reactivity to other antigens<sup>33,34</sup>. Therefore, we were surprised that BC2 was activated by several epidermal lipids with differing retention factors (Rfs) and chemical structures. For example, BC2 was activated by lipids in band 2, which comigrated with a free fatty acid standard (Fig 5b) and was demonstrated to contain free fatty acids by MS (Supplementary Fig. 4a). Also, fraction 3-4 was highly stimulatory, and comparison with standards demonstrated comigration with TAG or wax ester standards or both. MS analysis detected triglycerides in fraction 3 and fraction 3-4, and cholesterol esters were detected in fraction 4 (Supplementary Fig. 4b-d). Responses from purified epidermal extracts were compared to synthetic or natural standards to clarify the role of wax esters or cholesterol esters in stimulating the response and to evaluate the possibility that antigenicity resulted from trace contaminants in natural lipid samples. Analysis of synthetic molecules agreed with the results obtained from natural lipids: both showed that TAGs, wax esters and free fatty acids are autoantigens (Fig. 5b). Thus, several structurally related apolar antigens are produced in human epidermis. However, T cell responses to lipid structures were not extremely promiscuous: T cells did not recognize other equivalently hydrophobic molecules, such as cholesterol or cholesterol esters (Fig. 5b), or self lipids with hydrophilic head groups (Fig. 3b). Instead, T cells recognized three highly apolar classes of skin lipids, wax esters, TAG and fatty acids.

### Squalene is a sebaceous autoantigen

Skin repels microbes and retains water by creating surface barriers comprised of unusually hydrophobic lipids. Therefore, further studies sought to explain the high antigenicity of skin by pinpointing the source of antigenic lipids, and were guided by published evidence showing that apolar lipids naturally concentrate as extracellular lipids present in the stratum corneum and sebum<sup>31,35,36</sup>. Sebum is a natural mixture of apolar oils and waxy substances that are normally sequestered in sebaceous glands, and are therefore not directly accessible to epidermal compartments or CD1a<sup>+</sup> Langerhans cells. Sebum is secreted through hair follicle or sweat glands, where it normally coats the outermost skin surface. Using tissue microdissection to capture sebaceous glands (Fig. 6a), we analyzed the lipid content and antigenicity of sebum. In agreement with prior reports<sup>31,36</sup>, the lipid profile was strongly skewed toward hydrophobic lipids, with enrichment of TAG and wax esters. Also sebum is highly enriched in the apolar terpene, squalene (Fig. 6a)<sup>31</sup>. Human sebum from microdissected glands, as well as pure synthetic squalene, strongly activated BC2 (Fig. 6b). Squalene is an unsubstituted terpene lipid that lacks all polar functional groups, so identification of this antigen provides evidence for T cell activation by a compound with extreme apolarity.

### Headgroups block T cell activation

Crystal structures of CD1-lipid complexes show that lipid antigen recognition typically occurs by TCR interaction with charged or polar elements of amphipathic lipids<sup>14,18</sup>. In contrast, fatty acids (C16), wax esters (C36), triacylglycerides (C51) and squalene (C30) lacked highly polar head groups. Also, lipids identified here were cross-reactively recognized despite large differences in size. The observed patterns of cross-reactivity might be explained by a simple model that T cell activation occurs when CD1a is occupied by small hydrophobic antigens that are nested within the groove. Recognition does not require direct TCR contact with the antigen's headgroup, nor highly specific positioning of the antigen for TCR interaction. Instead such nested apolar lipids might affect CD1a conformation from an internal position or cause unloading of lipids whose bulky headgroups block the TCR approach to CD1a.

Building on initial results suggesting that certain lipid ligands of CD1a inhibit autoreactivity (Fig. 3d), we undertook more detailed studies to test the functions of headless and headed ligands of CD1a (Fig. 7a). First, to confirm that stimulatory lipids bind in the CD1a groove, we measured the extent to which recognition of squalene, wax ester and fatty acid recognition is blocked by CD1a pretreatment with DDM and sphingomyelin, which normally seat within one or two pockets of the CD1a groove<sup>18,37</sup>. In agreement with studies showing ready exchange of endogenous and exogenous lipids in cell surface CD1 proteins<sup>38</sup>, T cell activation was reduced or abolished in a dose dependent fashion when CD1a proteins were pretreated with increasing DDM or sphingomyelin. These results suggests exchange of lipopeptides or glycolipids for antigenic apolar lipids, as well as a specific inhibitory function of headed antigens (Fig. 7b). Further supporting this conclusion, many examples of CD1a ligands with phosphate, sulfate, carbohydrate, anionic or zwitterionic headgroups, which failed to activate BC2 in plate bound assays (Fig. 3b), also inhibited the autoreactivity to CD1a proteins under controlled conditions. Dose dependent inhibition was observed in all cases when headed ligands were applied to fresh cell-derived CD1a proteins or CD1a that was pre-stripped with acid (Fig. 7c). Overall, the skin-derived antigens activated T cells independently of all cofactors normally present in APCs. Antigens likely functioned through CD1a groove binding in a process that involved exchange of endogenous antigens with non-stimulatory lipids carrying bulky headgroups, including certain types of lipids identified here as being normally loaded into CD1a in cells.

## Structure-function studies of headgroup size

Next we studied lipids with small or absent headgroups, which were compared to lipids with the same or similar alkyl chains, but were modified to increase or decrease headgroup size and polarity. For example, fatty acids are partially charged, but the charge is absent in fatty alcohols or methyl esters. Although free fatty acids show detectable autoreactivity (Fig. 5b, 7d), blocking the carboxylate group by either strategy significantly increased antigenic potency, providing gain of function (Fig. 7d). The wax ester antigen, which contains a weakly polar internal ester, can be rendered more polar by adding a glycerol unit to create diacylglycerol, or by further addition of a phosphate group to create phosphodiacylglycerol. Activation is reduced when adding internal esters and free alcohol groups, and recognition is abrogated by a phosphate headgroup (Fig. 7e).

To determine whether the observed pattern of activation by hydrophobic headless lipids was a more general feature of CD1a-autoreactive T cells, we tested our initially generated T cell lines for activation by the identified activating ligands for BC2. Although Bgp and BC2 express differing TCRs (Supplementary Fig. 5) both recognized hydrophobic antigens and showed a similar overall hierarchy of recognition of individual antigens, although responses by Bgp were weaker (Fig. 7f). The weaker response by Bgp to all antigens may explain why in the initial screening with cell-derived truncated CD1a protein, we did not observe activation of this T cell line, even though autoreactivity to full length CD1a on cells is apparent (Fig. 1). In summary, contrary to previously known CD1 antigens, CD1a autoantigens are extremely apolar, oily substances, which are recognized based on their lack of polar head groups.

## Discussion

Antigens are typically positioned partly within CD1 or MHC grooves, yet rise up to the plane of TCR contact, creating a composite surface with that antigen presenting molecule, which is the TCR epitope<sup>12-14</sup>. The structural constraints of this type of ternary interaction correctly predict the observed molecular structures of the known antigens for  $\alpha\beta$  T cells: peptides and lipids generally match or exceed the molecular volume of the grooves they bind. These antigens contain polar atoms that mediate highly specific interactions with TCRs<sup>12-14</sup>. In contrast, squalene (C30), wax esters (C36), TAGs (C51) and fatty acids (C16) largely lack substrates for hydrogen bonding, and they are cross-reactively recognized despite substantial differences in their size. Notably, squalene, a relatively potent natural CD1a autoantigen, lacks any chemical basis for hydrogen bonding or charge-charge interactions with the TCR. The divergence of these newly discovered structures from previously identified  $\alpha\beta$  T cell antigens points toward a model for T cell activation whereby skin oils are recognized based on the antigen creating non-interference of an interaction of CD1a and the TCR.

A study of CD1d-reactive TCRs shows how autoreactivity can be blocked by addition of bulky lipid ligands<sup>39,40</sup>, similar to the inhibitory headed ligands of CD1a identified here. Also, CD1b binds small hydrophobic ligands wholly within the groove such that there is no extension to the outside of CD1b, where TCR interaction normally occurs<sup>25,41</sup>. Here we show that the natural ligands of CD1a are also small hydrophobic molecules, but unlike scaffold lipids in the CD1b system, these ligands activate T cells. In contrast to nonamer peptides or diacylglycerols that are of predictable size and match the volume constraints of their respective antigen binding groove, stimulatory compounds identified here range from C16 to C51. These antigens do not match each other in length, nor do they match the volume of the CD1a (1360 Å<sup>3</sup>), which is optimal for ~C42 lipids<sup>37</sup>. These cell free assays do not allow antigen processing, so the diverse sizes are likely maintained until the activating event. Therefore, it is unlikely that the T cell activation is mediated through a single type of



homogenous seating of antigens within the CD1a groove, as is typical of known antigens. TAGs somewhat exceed the expected volume of the CD1a groove (C42), so might be recognized through conformational adaptation of CD1a, or the lipid might protrude through the F' portal, as occurs for cardiolipin in CD1d<sup>42</sup>. Specifically, human CD1a has a notch in the lateral margin of the F' pocket, which might allow TAG might to escape laterally without crossing into the plane of TCR contact<sup>18</sup>.

Two non-exclusive models are that the apolar antigens stabilize the groove, or that they displace inhibitory ligands. There is evidence that internally positioned lipids alter the outer CD1 surfaces<sup>38,43</sup>. The loss of BC2 response after acid-stripping of CD1a proteins suggests that this mechanism is active. However, the dominant mechanism seems to be that apolar antigens displace CD1a ligands with bulky or charged headgroups, which would otherwise interfere with CD1a-TCR contact. Supporting noninterference, cellular CD1a proteins bind many ligands with large headgroups, and certain of these headed ligands block autoreactivity to CD1a. CD1a autoreactive T cell activation does not result from one potent agonist, but rather from the ratio of apolar to polar antigens bound to a cohort of CD1a proteins, so the mechanism is more like a rheostat than an on-off switch.

Skin oils represent natural tissue-specific autoantigens. The lipid profile of most tissues is dominated by membrane phospholipids and sphingolipids. Although TAG, fatty acids, squalene can be found in all cells, their extracellular accumulation is largely restricted to human sebaceous glands and cornified epithelia, which are also the locations where unusual wax esters are produced in large quantity<sup>31</sup>. Thus, lipid autoantigens are spatially distributed within defined extracellular subcompartments of the skin. CD1a expression is likewise largely restricted to epidermal LCs. These observations suggest a near neighbor model in which constitutive activation of T cells occurs. Trauma, infection or other barrier breaches could transfer surface skin oils to deeper layers, promoting CD1a autoreactive T cell response, including epithelial repair mechanisms associated with IL-22<sup>2,5</sup>.

Discovery of the antigenic properties of skin lipids provides candidate mechanisms by which alterations in lipid content might influence disease. For example, atopic dermatitis and psoriasis are associated with changes in ceramide or other skin lipid composition<sup>44,45</sup>, and treatments to alleviate symptoms include ointments containing lipids that are shown here to affect T cell response<sup>46</sup>. Also, T cell response to hydrophobic components of oils provides a candidate mechanism for understanding the action of hydrophobic skin contact sensitizers, which activate T cells but do so by unknown mechanisms. Finally, squalene is a major component of two adjuvants, MF59 and AS03, which are used in influenza vaccines in Europe, but whose mechanisms are not fully known<sup>47</sup>. Thus, CD1a antigen presentation represents a new candidate mechanism for adjuvancy.

## On-Methods

### Reagents

Lipid standards were purchased from commercial sources. Cholesterol (catalog#: C8667), cholesterol ester (catalog#: C6072), Lauryl palmitoleate (wax ester, catalog#: P1642), triacylglycerol (TAG, glycerol trioleate, catalog#: T7140; glycerol tripalmitoleate, catalog#: T2630), palmitoleic acid (fatty acid, catalog#: P9417), palmitoleyl alcohol (fatty alcohol, catalog#: P1547), methyl palmitoleate (fatty methyl ester, catalog#: P9667), squalene (catalog#: S3626), monosialoganglioside (GM3, catalog#: G5642) were purchased from Sigma-Aldrich. C18 Ceramide (Cer, catalog#: 860518), C16  $\beta$ -D-glucosyl ceramide (GluCer, catalog#: 860539), C24  $\beta$ -D-lactosyl ceramide (Lac-cer, catalog#: 860577), phosphatidylcholine (PC, catalog#: 770365), Lyso-PC (LPC, catalog#: 855810), phosphatidylinositol (PI, catalog#: 850144), phosphatidylglycerol (PG, catalog#: 840503),

phosphatidylethanolamine (PE, catalog#: 850757), phosphatidylserine (PS, catalog#: 840032), phosphatidic acid (PA, catalog#: 840857), sphingomyelin (SM, catalog#: 860584), 1-palmitoyl-2-oleoyl-sn-glycerol (DAG, catalog#: 800815) were purchased from Avanti polar lipids. Sulfatide (catalog#:1049), Ceramide trihexosides (Gb3, catalog#: 1067), and Globotetrahexosylceramide (Gb4, catalog#: 1068) were purchased from Matreya. Oleyl palmitoleate (wax ester, catalog#: WE1404) and Oleyl oleate (wax ester, catalog#: WE1405) were purchased from Nu-Chek.

### Cellular assays

CD1a autoreactive T cell lines cell cultures were co-cultured with APCs (mock-transfected K562 cells, CD1-transfected K562 cells) for 24 h and supernatant was analyzed for IL-2, by HT-2 bioassay or IFN- $\gamma$  ELISA. For blocking experiments, CD1-transfected K562 cells were preincubated for 1 h at 37 °C with blocking antibody to the corresponding CD1 molecule, including OKT-6 (anti-CD1a), BCD1b3.1 (anti-CD1b), F10/21A3 (anti-CD1c), CD1d42 (anti-CD1d), and or P3 (control IgG) (10  $\mu$ g/ml) before adding T cells.

### Recombinant CD1 protein and lipid eluates

Soluble biotinylated CD1 proteins was produced in lentivirus-transduced HEK293 cells by the National Institutes of Health Tetramer Core Facility (Emory University, Atlanta, GA). Generation and purification of CD1a protein is similar to CD1b protein, which has been described previously<sup>16</sup>. CD1 and control proteins (MHC-I) were magnetic capture by streptavidin Dynabeads (Invitrogen), immobilized proteins were washed three times with PBS and extracted successively with chloroform/methanol (1:2, and 2:1). Elutes from proteins were separated from beads by centrifugation, which were then stored at -20 °C.

### Plate binding assay

96-well streptavidin plates (Thermo Scientific) were incubated for 24 h at room temperature with 0.5  $\mu$ g of CD1a protein and 125 ng anti-CD1a (AbD Serotec) per well in PBS, pH 7.4. Plates were then washed with PBS three times (200  $\mu$ l/well) and antigens were sonicated in PBS for 2 minutes and added to the wells and incubated at room temperature for 24–40 hours. The plates were washed with PBS three times before adding  $10^5$  T cells in a total volume of 200  $\mu$ l of T cell medium per well. The plates were then incubated for 24 h at 37 °C, after which culture supernatants were collected for IFN- $\gamma$  ELISA analysis (Thermo Scientific). For the acid strip protocol, after 24 h coating of protein, the plates were washed with PBS three times followed by citrate buffer (pH 3.4 or indicated pH) wash (200  $\mu$ l/well, 10 minute incubation twice) and three PBS washes before adding lipid antigens.

### Epidermis, sebaceous gland and thyroid gland isolation

Discarded human thyroid tissues were obtained from thyroidectomy specimens resected from patients with autoimmune thyroiditis with the approval of the Institutional Review Board of Partners Human Research Committee. Normal human skin samples were obtained as discarded material after cosmetic surgery under approved protocol of the Institutional Review Board of Partners Human Research Committee. Occipital scalp samples were obtained as discarded tissue during hair transplantation surgery, and were designated as nonhuman subject research under 45 CFR Part 46. We therefore received an Institutional Review Board exemption at Columbia University to use these materials. Epidermis was separated from dermis as previously described<sup>48</sup> and sebaceous glands were isolated using tissue microdissection methods.

## Lipid extraction

For cells, culture media was removed and cells were washed with PBS twice. Cell pellets were extracted successively with chloroform/methanol (1:2 and 2:1) for 2 hours. Supernatants from two extractions were combined and dried under nitrogen gas. Lipids were weighted and stored in Chloroform/methanol at  $-20^{\circ}\text{C}$ . Lipid extraction from epidermis and thyroid tissues was similar procedure as described above except that the samples were homogenized before solvent extraction. Alternatively, samples were extracted with chloroform only.

## Lipid purification by Thin Layer Chromatography

Silica-coated glass TLC plates (10×20 cm or 20×20 cm, Scientific Adsorbents Incorporated, GA) were used for analytical or preparative lipid separation. Plates were pre-cleared in chloroform/methanol/water (60/30/6, V/V/V) to remove contaminants on the plates. The lipids extracts (100  $\mu\text{g}$ ) were developed with a single (hexane/diethyl ether/acetic acid (70/30/1, V/V/V)<sup>32</sup>, dual (1<sup>st</sup>: chloroform/methanol/water (60/35/8, V/V/V) 60% height from the origin, and 2<sup>nd</sup>: hexane/diethyl ether/acetic acid (70/30/1, V/V/V) to the top)<sup>32</sup>, or triple solvent system (1<sup>st</sup>: n-hexane/benzene (50/50, V/V) to the top, 2<sup>nd</sup>: chloroform/methanol/water (60/16/2, V/V/V) to 5 cm from the origin, 3<sup>rd</sup>: hexane/diethyl ether/acetic acid (80/20/10, V/V/V) to 12 cm from the origin) (method modified from <sup>49</sup>). To visualize the spots, plates were sprayed with a solution of 3% (w/v) of cupric acetate in 8% (V/V) of phosphoric acid, followed by heating at  $150^{\circ}\text{C}$  for 20–30 min. Chloroform extracted skin lipids (4 mg) were loaded on a 20×20 TLC plate as a 10 cm-band and 25  $\mu\text{g}$  of lipid extracts were spotted on the same plate for later charring. After the plate was developed in the solvent system of hexane/diethyl ether/acetic acid (70/30/1, V/V/V), the plate was separated to two pieces. The piece containing 25  $\mu\text{g}$  of material was charred for the reference and another piece containing 4 mg was scraped according to the reference spots. The intervals between bands were also scraped. The silica was extracted with two times of chloroform/methanol (2:1).

## Mass spectrometry and identification of self lipids of recombinant CD1a by ESI-MS and HPLC-MS

For nanoelectrospray analysis, 4  $\mu\text{g}$  of protein was denatured and extracted with 100  $\mu\text{l}$  methanol, 10  $\mu\text{L}$  of unseparated mixtures were loaded onto an in-house made glass nanospray tip for both positive- and negative-mode electrospray ionization mass spectrometry (ESI-MS). The ESI-MS and collision induced dissociation (CID-MS/MS) were performed on LCQ Advantage or LXQ (Thermo Finnigan, Ringoes, NJ), 2 dimensional ion-trap mass spectrometers. The spray voltage and capillary temperature were set to 0.8 kV and  $200^{\circ}\text{C}$ , respectively. Collision energy was 30 – 40 % of maximum and the trapping of product ions were carried out with a  $q$  value of 0.25. HPLC-MS and lipidomics analysis of CD1a eluted lipids was performed as previously described <sup>25</sup>. Briefly, extracted lipid ligands were analyzed with an Agilent Technologies 6520 Accurate-Mass Q-TOF coupled with an Agilent 1200 series HPLC system controlled by MassHunter software as described <sup>28</sup>

## Expression, refolding and purification of recombinant TCRs

The BC2 TCR was produced following protocols previously described <sup>50</sup>. Briefly, individual  $\alpha$  and  $\beta$  chains of the TCR, with an engineered disulfide bond between the TRAC and TRBC constant domains, were expressed in BL21 E. coli cells as inclusion bodies and solubilised in 8 M urea buffer containing 10 mM Tris-HCl pH 8, 0.5 mM Na-EDTA, and 1 mM dithiothreitol. The TCR was then refolded in refolding buffer that was comprised of 5M urea, 100 mM Tris-HCl pH 8, 2 mM Na-EDTA, 400 mM L-Arg-HCl, 0.5 mM oxidized glutathione and 5 mM reduced glutathione. The refolded solution was dialyzed twice against

10 mM Tris-HCl pH 8.0 overnight to allow sufficient buffer exchange. The dialyzed samples were then purified through DEAE cellulose, size-exclusion and anion exchange HiTrap Q chromatography approaches. The quality and purity of the samples were analyzed via SDS-PAGE.

### Surface Plasmon resonance

Biotinylated CD1a-endogenous lipid derived from the mammalian expression system (HEK293 cells as described above) was coupled to research-grade streptavidin-coated chips to a mass concentration of ~2000 resonance units. Increasing concentrations of the BC2 TCR (0–200  $\mu$ M) were injected over all flow cells for 30 s at a rate of 5  $\mu$ l/min at 25 °C on a Biacore 3000 in 10 mM Tris-HCl pH 8, 150 mM NaCl buffer. The final response was calculated by subtraction of the response for CD1a-endogenous minus an empty flow cell containing biotin only. The  $R_{max}$  value indicated that 9.5% of the CD1a-endogenous complex was reactive against BC2 TCR. The data were fitted to a 1:1 Langmuir binding model using BIAevaluation version 3.1 software (Biacore AB) and the equilibrium data analyzed using Prism program for biostatistics, curve fitting and scientific graphing (GraphPad).

### Accession codes

Genbank: TCR  $\alpha$ - and  $\beta$ -chains of BC2 and Bgp KF751594, KF751595, KF751596, KF751597

### Supplementary Material

Refer to Web version on PubMed Central for supplementary material.

### Acknowledgments

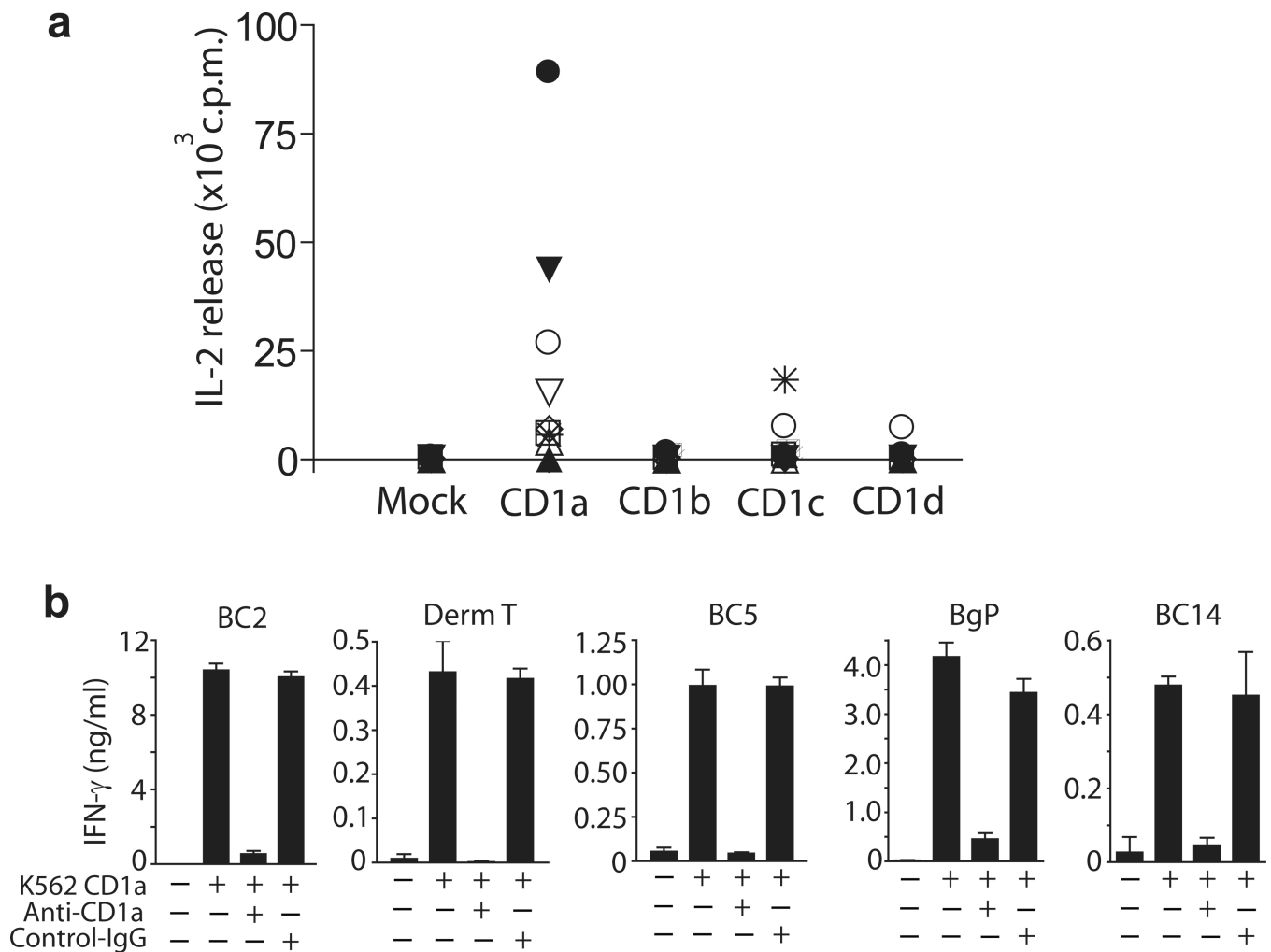
We thank Dr. T. Hansen for providing protein expression vector and the HLA-B2705 gene template. We thank Dr. C. Higgins for the photo of the sebaceous glands. This project was supported by the Burroughs Wellcome Fund (to D.B.M.), the Mizutani Foundation and the NIH (AR R01048632, AI 049313 to D.B.M.) and by a Research Career Development Award from the Dermatology Foundation (A.d.J.) and a Research grant from the American Skin Association (A.d.J), and the NIH Tetramer Facility contract (HHSN272201300006C) to J.D.A. S.G. is supported by an Australian Research Council Future Fellowship and J.R. is supported by an National Health and Medical Research Council Australia Fellowship. We thank L.L. Tan for technical support for the BC2 TCR production, and we thank the members of the NIH Tetramer Facility for preparation of CD1a.

### References

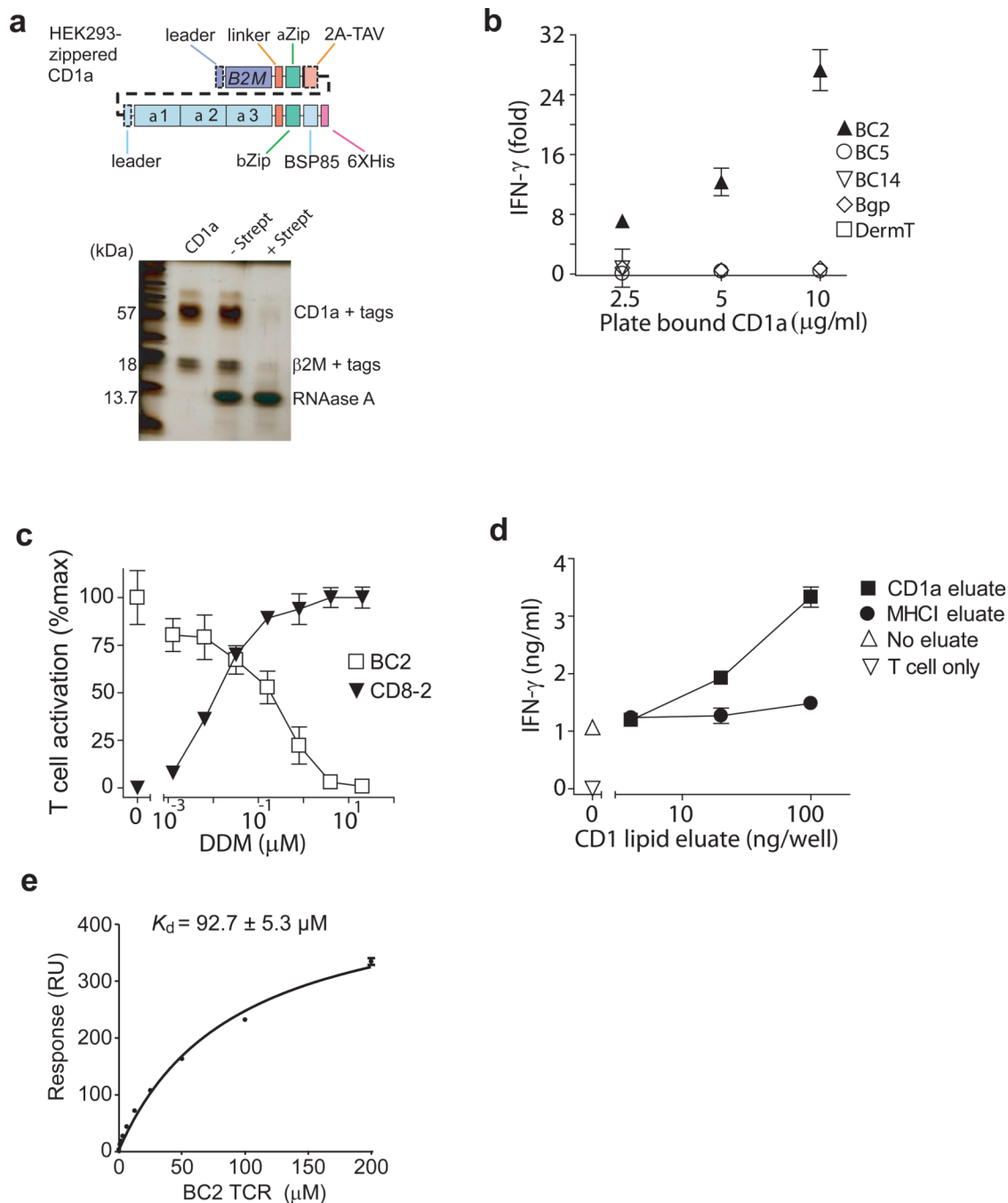
1. Porcelli S, et al. Recognition of cluster of differentiation 1 antigens by human CD4-CD8-cytolytic T lymphocytes. *Nature*. 1989; 341:447–450. [PubMed: 2477705]
2. de Jong A, et al. CD1a-autoreactive T cells are a normal component of the human alphabeta T cell repertoire. *Nature immunology*. 2010; 11:1102–1109. [PubMed: 21037579]
3. de Lalla C, et al. High-frequency and adaptive-like dynamics of human CD1 self-reactive T cells. *European journal of immunology*. 2011; 41:602–610. [PubMed: 21246542]
4. Roura-Mir C, et al. CD1a and CD1c activate intrathyroidal T cells during Graves' disease and Hashimoto's thyroiditis. *Journal of immunology*. 2005; 174:3773–3780.
5. Colonna M. Skin function for human CD1a-reactive T cells. *Nature immunology*. 2010; 11:1079–1080. [PubMed: 21079630]
6. Shamshiev A, et al. Self glycolipids as T-cell autoantigens. *European journal of immunology*. 1999; 29:1667–1675. [PubMed: 10359121]
7. Zhou D, et al. Lysosomal glycosphingolipid recognition by NKT cells. *Science*. 2004; 306:1786–1789. [PubMed: 15539565]

8. Mattner J, et al. Exogenous and endogenous glycolipid antigens activate NKT cells during microbial infections. *Nature*. 2005; 434:525–529. [PubMed: 15791258]
9. Fox LM, et al. Recognition of lyso-phospholipids by human natural killer T lymphocytes. *PLoS biology*. 2009; 7:e1000228. [PubMed: 19859526]
10. Brennan PJ, et al. Invariant natural killer T cells recognize lipid self antigen induced by microbial danger signals. *Nature immunology*. 2011; 12:1202–1211. [PubMed: 22037601]
11. Van Rhijn I, et al. CD1d-restricted T cell activation by nonlipidic small molecules. *Proceedings of the National Academy of Sciences of the United States of America*. 2004; 101:13578–13583. [PubMed: 15342907]
12. Garboczi DN, et al. Structure of the complex between human T-cell receptor, viral peptide and HLA-A2. *Nature*. 1996; 384:134–141. [PubMed: 8906788]
13. Garcia KC, et al. An alphabeta T cell receptor structure at 2.5 Å and its orientation in the TCR-MHC complex. *Science*. 1996; 274:209–219. [PubMed: 8824178]
14. Borg NA, et al. CD1d-lipid-antigen recognition by the semi-invariant NKT T-cell receptor. *Nature*. 2007; 448:44–49. [PubMed: 17581592]
15. Altman JD, et al. Phenotypic analysis of antigen-specific T lymphocytes. *Science*. 1996; 274:94–96. [PubMed: 8810254]
16. Kasmar AG, et al. CD1b tetramers bind alphabeta T cell receptors to identify a mycobacterial glycolipid-reactive T cell repertoire in humans. *The Journal of experimental medicine*. 2011; 208:1741–1747. [PubMed: 21807869]
17. Porcelli SA. The CD1 family: a third lineage of antigen-presenting molecules. *Advances in immunology*. 1995; 59:1–98. [PubMed: 7484459]
18. Zajonc DM, et al. Molecular mechanism of lipopeptide presentation by CD1a. *Immunity*. 2005; 22:209–219. [PubMed: 15723809]
19. Moody DB, et al. T cell activation by lipopeptide antigens. *Science*. 2004; 303:527–531. [PubMed: 14739458]
20. Ernst WA, et al. Molecular interaction of CD1b with lipoglycan antigens. *Immunity*. 1998; 8:331–340. [PubMed: 9529150]
21. Deng L, Mariuzza RA. Recognition of self-peptide-MHC complexes by autoimmune T-cell receptors. *Trends in biochemical sciences*. 2007; 32:500–508. [PubMed: 17950605]
22. Cox D, et al. Determination of cellular lipids bound to human CD1d molecules. *PLoS one*. 2009; 4:e5325. [PubMed: 19415116]
23. Yuan W, Kang SJ, Evans JE, Cresswell P. Natural lipid ligands associated with human CD1d targeted to different subcellular compartments. *Journal of immunology*. 2009; 182:4784–4791.
24. Haig NA, et al. Identification of self-lipids presented by CD1c and CD1d proteins. *The Journal of biological chemistry*. 2011; 286:37692–37701. [PubMed: 21900247]
25. Huang S, et al. Discovery of deoxyceramides and diacylglycerols as CD1b scaffold lipids among diverse groove-blocking lipids of the human CD1 system. *Proceedings of the National Academy of Sciences of the United States of America*. 2011; 108:19335–19340. [PubMed: 22087000]
26. Sugita M, et al. Separate pathways for antigen presentation by CD1 molecules. *Immunity*. 1999; 11:743–752. [PubMed: 10626896]
27. Barral DC, et al. CD1a and MHC class I follow a similar endocytic recycling pathway. *Traffic*. 2008; 9:1446–1457. [PubMed: 18564371]
28. Layre E, et al. A comparative lipidomics platform for chemotaxonomic analysis of *Mycobacterium tuberculosis*. *Chemistry & biology*. 2011; 18:1537–1549. [PubMed: 22195556]
29. Murphy GF, Bhan AK, Sato S, Mihm MC Jr, Harrist TJ. A new immunologic marker for human Langerhans cells. *The New England journal of medicine*. 1981; 304:791–792. [PubMed: 6970334]
30. Crozat K, et al. Comparative genomics as a tool to reveal functional equivalences between human and mouse dendritic cell subsets. *Immunological reviews*. 2010; 234:177–198. [PubMed: 20193019]
31. Nicolaides N. Skin lipids: their biochemical uniqueness. *Science*. 1974; 186:19–26. [PubMed: 4607408]

32. Touchstone JC. Thin-layer chromatographic procedures for lipid separation. *Journal of chromatography. B, Biomedical applications*. 1995; 671:169–195.
33. Moody DB, et al. Structural requirements for glycolipid antigen recognition by CD1b-restricted T cells. *Science*. 1997; 278:283–286. [PubMed: 9323206]
34. de Jong A, et al. CD1c presentation of synthetic glycolipid antigens with foreign alkyl branching motifs. *Chemistry & biology*. 2007; 14:1232–1242. [PubMed: 18022562]
35. Lampe MA, et al. Human stratum corneum lipids: characterization and regional variations. *Journal of lipid research*. 1983; 24:120–130. [PubMed: 6833889]
36. Kellum RE. Human sebaceous gland lipids. Analysis by thin-layer chromatography. *Archives of dermatology*. 1967; 95:218–220. [PubMed: 6019001]
37. Zajonc DM, Elsliger MA, Teyton L, Wilson IA. Crystal structure of CD1a in complex with a sulfatide self antigen at a resolution of 2.15 Å. *Nature immunology*. 2003; 4:808–815. [PubMed: 12833155]
38. Manolova V, et al. Functional CD1a is stabilized by exogenous lipids. *European journal of immunology*. 2006; 36:1083–1092. [PubMed: 16598820]
39. Mallevaey T, et al. A molecular basis for NKT cell recognition of CD1d-self-antigen. *Immunity*. 2011; 34:315–326. [PubMed: 21376640]
40. Rossjohn J, Pellicci DG, Patel O, Gapin L, Godfrey DI. Recognition of CD1d-restricted antigens by natural killer T cells. *Nature reviews. Immunology*. 2012; 12:845–857.
41. Garcia-Alles LF, et al. Endogenous phosphatidylcholine and a long spacer ligand stabilize the lipid-binding groove of CD1b. *The EMBO journal*. 2006; 25:3684–3692. [PubMed: 16874306]
42. Dieude M, et al. Cardiolipin binds to CD1d and stimulates CD1d-restricted gammadelta T cells in the normal murine repertoire. *Journal of immunology*. 2011; 186:4771–4781.
43. McCarthy C, et al. The length of lipids bound to human CD1d molecules modulates the affinity of NKT cell TCR and the threshold of NKT cell activation. *The Journal of experimental medicine*. 2007; 204:1131–1144. [PubMed: 17485514]
44. Di Nardo A, Wertz P, Giannetti A, Seidenari S. Ceramide and cholesterol composition of the skin of patients with atopic dermatitis. *Acta dermato-venereologica*. 1998; 78:27–30. [PubMed: 9498022]
45. Motta S, et al. Ceramide composition of the psoriatic scale. *Biochimica et biophysica acta*. 1993; 1182:147–151. [PubMed: 8357845]
46. Kircik LH, Del Rosso JQ, Aversa D. Evaluating Clinical Use of a Ceramide-dominant, Physiologic Lipid-based Topical Emulsion for Atopic Dermatitis. *The Journal of clinical and aesthetic dermatology*. 2011; 4:34–40. [PubMed: 21464885]
47. O'Hagan DT, Ott GS, De Gregorio E, Seubert A. The mechanism of action of MF59 - an innately attractive adjuvant formulation. *Vaccine*. 2012; 30:4341–4348. [PubMed: 22682289]
48. Pena-Cruz V, et al. Extraction of human Langerhans cells: a method for isolation of epidermis-resident dendritic cells. *Journal of immunological methods*. 2001; 255:83–91. [PubMed: 11470289]
49. Tachi M, Iwamori M. Mass spectrometric characterization of cholesterol esters and wax esters in epidermis of fetal, adult and keloidal human skin. *Experimental dermatology*. 2008; 17:318–323. [PubMed: 17979971]
50. Gras S, et al. The shaping of T cell receptor recognition by self-tolerance. *Immunity*. 2009; 30:193–203. [PubMed: 19167249]



**Figure 1.** CD1a-dependent activation of T cell lines. **(a)** IL-2 release by T cell cultures, measured by HT2 bioassay after 24 h of incubation with K562 cells transfected with CD1a, CD1b, CD1c, CD1d or empty vector (Mock). **(b)** IFN- $\gamma$  was measured by ELISA after 24 h with K562 CD1a cells, which were pre-treated (10  $\mu$ g/ml) with control IgG (P3) or anti-CD1a (OKT6). Results are representative of at least 3 experiments, which show the mean of triplicate measurements  $\pm$  standard deviation.

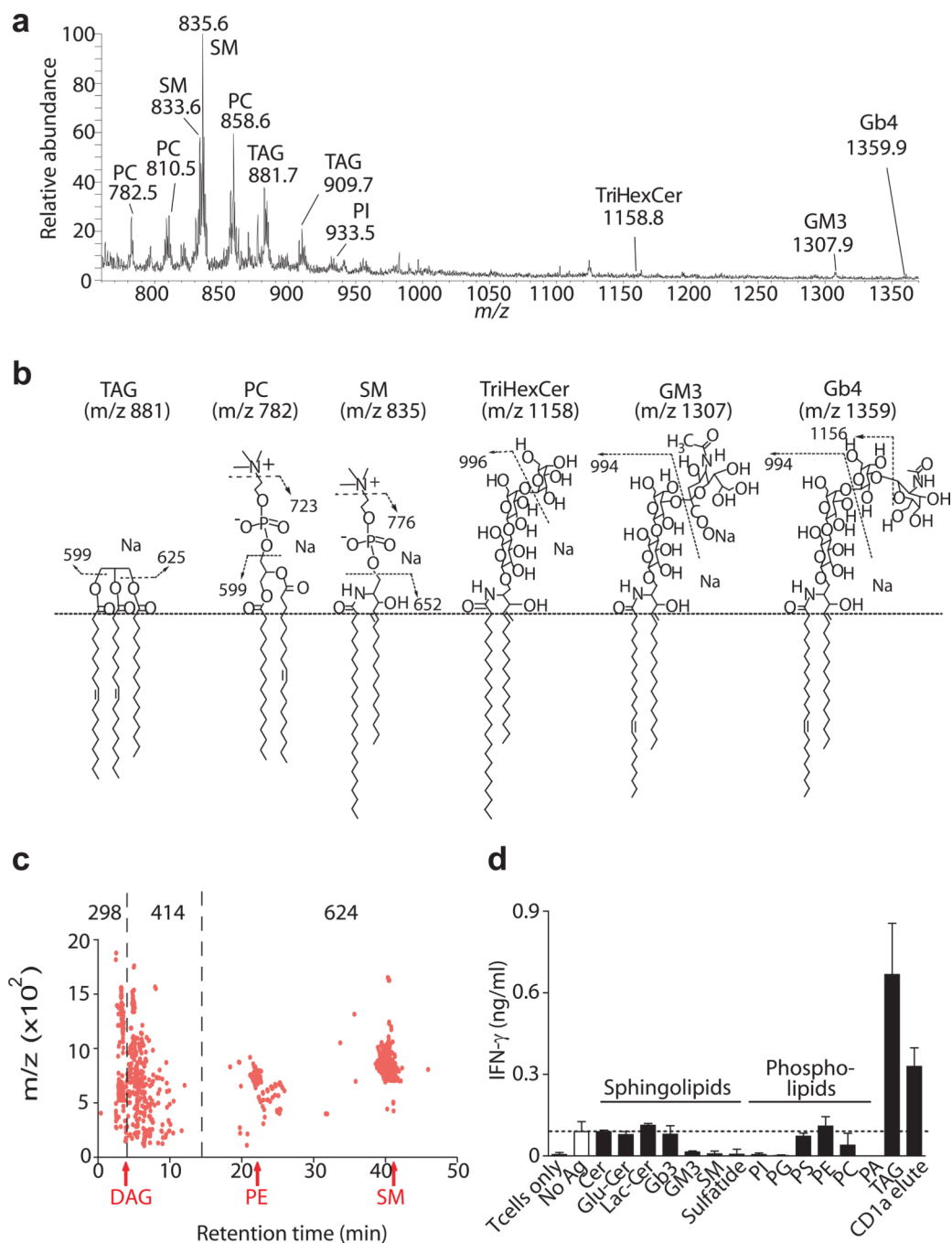


**Figure 2.**

Activation of CD1a-autoreactive T cell line by recombinant CD1a. **(a)** Schematics of engineered CD1 molecules show zipper-encoding regions ( $\alpha$ Zip and  $\beta$ Zip) and human *B2M* sequences, which are linked by cleavable 2A peptide from *Thosea asigna* virus (2A-TAV). Regions cleaved upon maturation (dashed line) and the biotinylation site (BSP85) are indicated. After depletion by agarose beads with and without streptavidin (Strept), CD1a was analyzed by polyacrylamide gel electrophoresis and silver staining. **(b)** CD1a protein was coated on streptavidin plates and incubated with CD1a-autoreactive T cell lines for 24 hrs. IFN- $\gamma$  ELISA results were plotted as the fold-increase of IFN- $\gamma$  production over

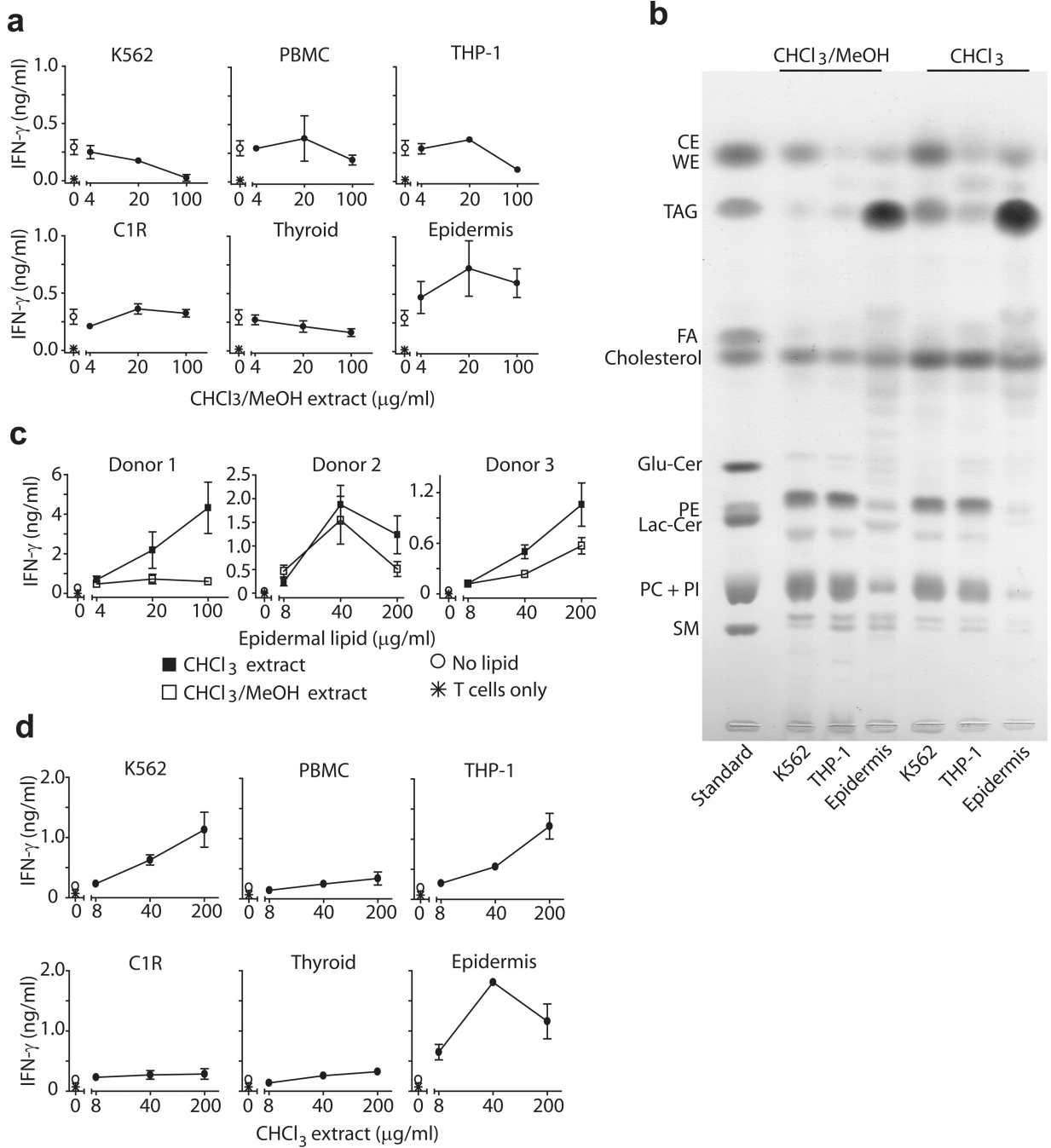


background. **(c)** Plate-bound CD1a protein was pulsed with DDM, then incubated with BC2 cell line or CD8-2 cell line and incubated for 24 h after which IFN- $\gamma$  was measured by ELISA. T cell activation was calculated as percentage of maximal IFN- $\gamma$  production of indicated T cell line. **(d)** Lipids eluted from recombinant CD1a and MHC class I protein (HLA-B2705) were pulsed onto plate-bound CD1a protein. Activation of BC2 cell line was measured after 24 h by IFN- $\gamma$  ELISA. Results are representative of 3 experiments, and depicted as the mean of triplicate measurements  $\pm$  standard deviation. **(e)** Surface Plasmon Resonance measurements of soluble BC2 TCR and immobilized, cell-derived CD1a monomers are representative of two experiments and are shown as the mean  $\pm$  standard error of the mean.

**Figure 3.**

Lipid composition of eluate from CD1a protein. **(a)** Chloroform and methanol eluents were subject to electrospray ionization-MS in positive mode. Detected compounds: Phosphatidylcholine (PC), Sphingomyelin (SM), Triacylglycerol (TAG), Phosphatidylinositol (PI), Trihexosylceramide (TriHexCer), Monosialoganglioside (GM3), Globotetrahexosylceramide (Gb4) **(b)** Lipid identifications are summarized with key identifying fragments shown. Full CID-MS spectra are shown in Supplementary Fig. 2 and 3. **(c)** CD1a proteins were extracted in chloroform and methanol, loaded into a silica-diol column and eluted in the normal phase. Individual events are assigned when signal is

detected in two or more replicate runs reproducibly detected within mass (20 ppm) and time (30 sec) windows. Retention time of all events (1,336) is divided into three retention time ranges that include lipids with low ( $n=298$ ), intermediate ( $n=414$ ) and high ( $n=624$ ) polarity, shown in comparison to known benchmark lipids, diacylglycerol (DAG), PI, phosphatidyl ethanolamine (PE) and sphingomyelin (SM). **(d)** Purified lipids or CD1a eluates were loaded onto plate-bound CD1a proteins that had been previously treated with acidic citrate buffer and tested for activation of BC2. Ceramide (Cer), Glucosylceramide (GluCer), Lactosylceramide (LacCer), Globotriaosylceramide (Gb3), phosphatidylglycerol (PG), phosphatidylserine (PS), phosphatidic acid (PA). Results are representative of at least 3 experiments, and depicted as the mean of triplicate measurements  $\pm$  standard deviation.

**Figure 4.**

Non-polar lipid extracts activate CD1a-autoreactive T cell line. **(a)** Lipids extracted from different cell types or tissues in chloroform (CHCl<sub>3</sub>) and methanol (MeOH) were pulsed onto recombinant plate-bound CD1a proteins leading to activation of BC2. **(b)** Lipids (100  $\mu$ g) extracted with CHCl<sub>3</sub>: MeOH (2:1, V:V) or CHCl<sub>3</sub> alone were analyzed by thin layer chromatography, compared to lipid standards and visualized by charring. Glucosylceramide (GluCer), fatty acids (FA), waxester (WE), cholesterol ester (CE). **(c,d)** Lipids extracted from epidermis **(c)** or other tissues **(d)** using CHCl<sub>3</sub>: MeOH (2:1, V:V) or CHCl<sub>3</sub> alone **(d)** were pulsed on recombinant plate-bound CD1a previously stripped with acidic citrate

buffer. Results are representative of 3 experiments, and depicted as the mean of triplicate measurements  $\pm$  standard deviation.

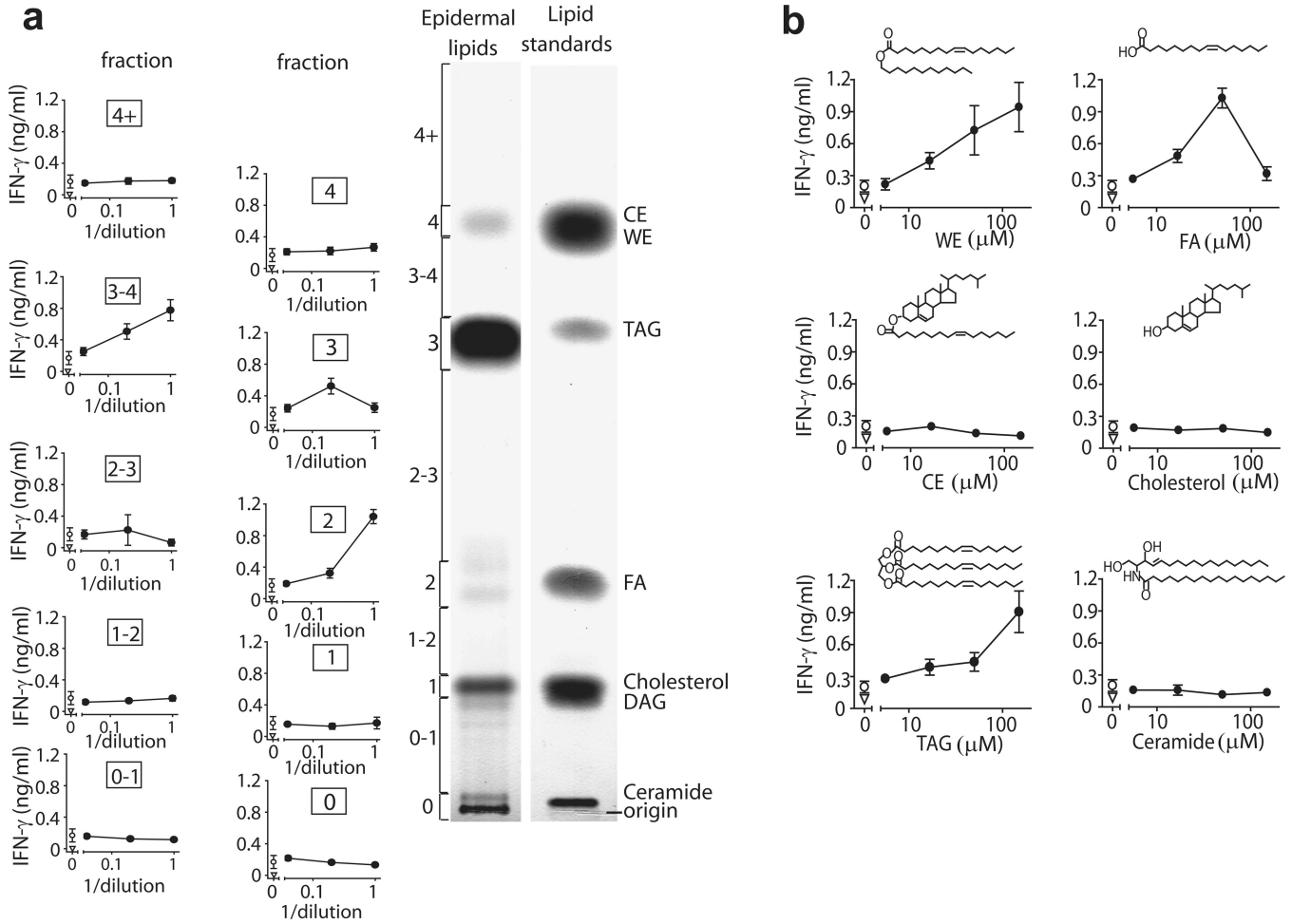


**Figure 5.** Human epidermis contains multiple lipid antigens. **(a)** Human epidermis was extracted by  $\text{CHCl}_3$ , and lipids were separated into 10 fractions (0, 0-1, 1, 1-2, 2, 2-3, 3, 3-4, 4, 4+) by normal phase preparative TLC in comparison to the named standards. IFN- $\gamma$  was measured by ELISA in supernatants of BC2 T cell line incubated with plate-bound CD1a loaded with dilutions of TLC extracted lipid fractions **(b)** Epidermal or purified synthetic lipids were loaded into citrate buffer stripped CD1a proteins and IFN- $\gamma$  release by BC2 was measured by ELISA. Wax ester (WE), fatty acid (FA), triacylglycerol (TAG). Results are representative of at least 3 experiments, and depicted as the mean of triplicate measurements  $\pm$  standard deviation.

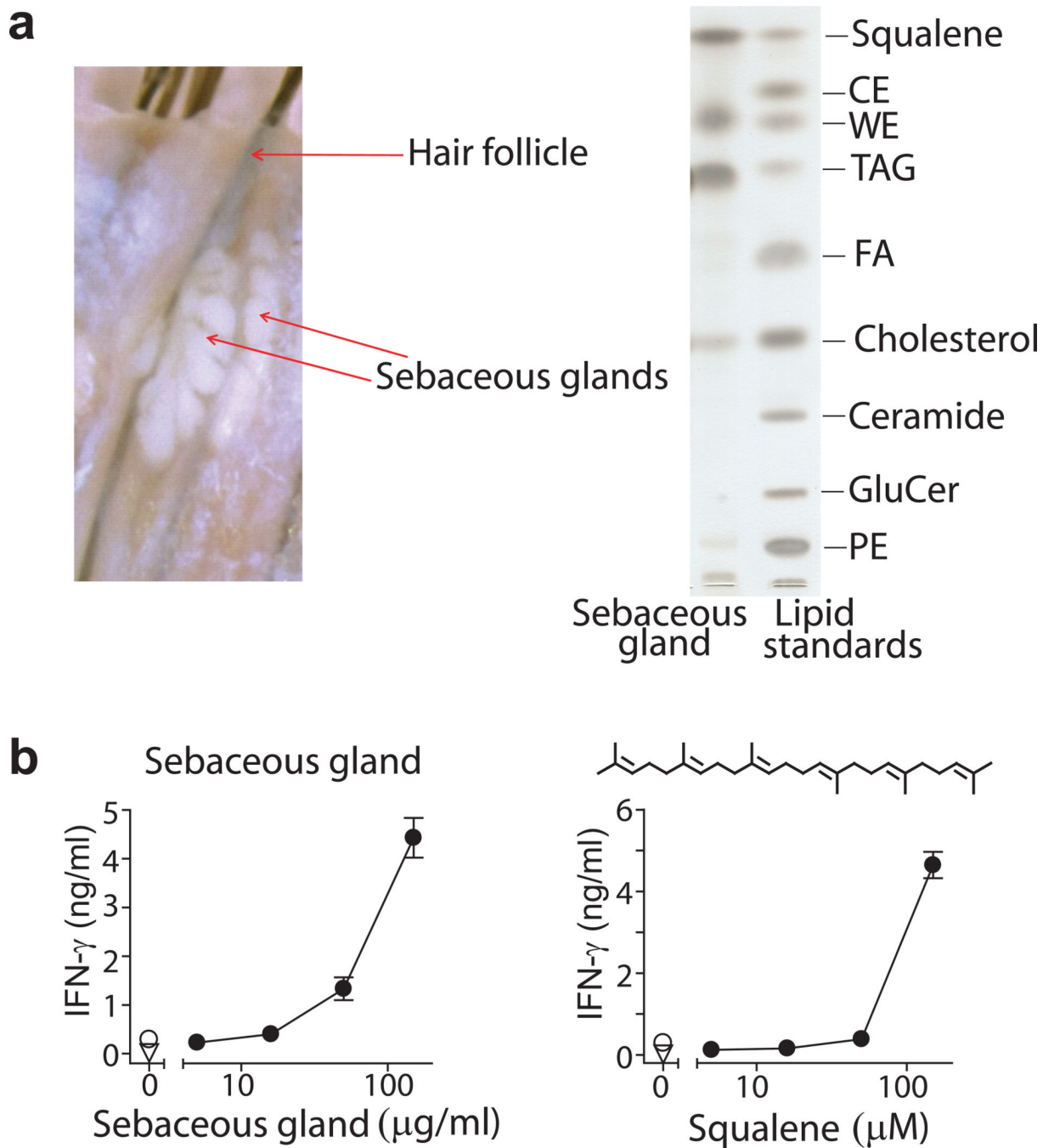


**Figure 6.**

Human sebaceous gland contains headless CD1a lipid antigens. **(a)** Sebaceous glands were microdissected from human occipital scalp tissue and lipids were isolated by chloroform extraction and analyzed by TLC. **(b)** Sebaceous gland lipids or synthetic squalene were loaded onto citrate buffer stripped, plate-bound CD1a proteins and tested for activation of BC2 by IFN- $\gamma$  ELISA. Results are representative of 3 experiments, and depicted as the mean of triplicate measurements  $\pm$  standard deviation.

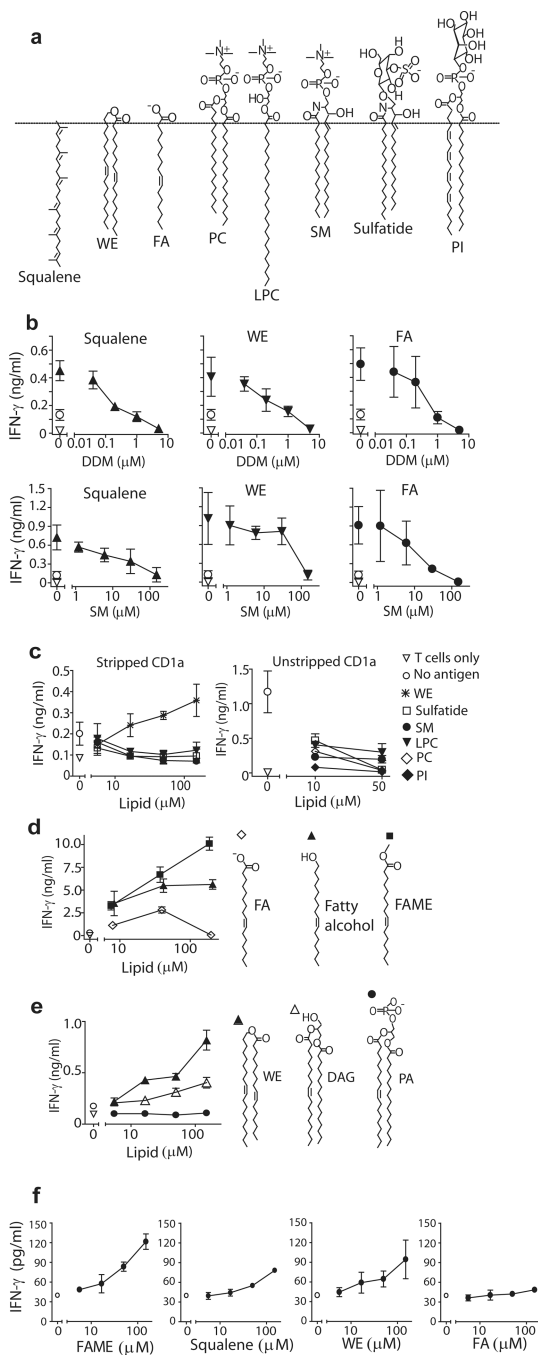


**Figure 7.** Hydrophilic head groups block CD1a antigen recognition. **(a)** Structures of identified activating and inhibitory lipids. Lysophosphatidylcholine (LPC) **(b)** CD1a protein was incubated with the indicated DDM or sphingomyelin concentration before squalene (50  $\mu$ M), wax ester (50  $\mu$ M) or fatty acid (50  $\mu$ M) was added. After 24 h coincubation followed by washing, BC2 was added and IFN- $\gamma$  release was measured by ELISA. **(c,d,e)** Indicated lipids were pulsed onto plate-bound CD1a protein. Activation of BC2 was measured after 24 h in the supernatant by IFN- $\gamma$  ELISA. **(f)** CD1a-autoreactive T cell line, Bgp, was tested for activation by the identified lipid antigens loaded onto plate-bound CD1a. IFN- $\gamma$  was



measured in the supernatant by ELISA. Results are representative of 3 experiments, and depicted as the mean of triplicate measurements  $\pm$  standard deviation.